

Optimum design of 3D reinforced concrete frames using IPGO algorithm

Ali Kaveh (✉ alikaveh@iust.ac.ir)

Iran University of Science & Technology <https://orcid.org/0000-0002-5428-4788>

Shaylin Rezazadeh Ardebili

Iran University of Science and Technology

Research Article

Keywords: 3D Reinforced concrete frames, Structural optimization, Improved plasma generation optimization (IPGO) algorithm, Metaheuristics

Posted Date: June 7th, 2022

DOI: <https://doi.org/10.21203/rs.3.rs-1507625/v1>

License: © ⓘ This work is licensed under a Creative Commons Attribution 4.0 International License.

[Read Full License](#)

Optimum design of 3D reinforced concrete frames using IPGO algorithm

Ali Kaveh* and Shaylin Rezazadeh Ardebili

*School of Civil Engineering, Iran University of Science and Technology, Narmak,
Tehran, P.O. Box 16846-13114, Iran*

Abstract

In this paper, optimum design of three-dimensional (3D) multi-story reinforced concrete (RC) structures is obtained using an improved version of the plasma generation optimization (IPGO) algorithm. The reinforcing bars and geometry of the cross-sections are considered as discrete variables that are chosen from a prearranged section database. The objective function is obtained from the cost of the framework, steel and concrete. The moment and shear frames are selected to design according to the American Concrete Institute's Building Code (ACI 318-8) requirements. The effectiveness of the proposed algorithm is investigated in the optimum design of 3D RC frames subjected to lateral seismic forces according to ASCE 7 requirements. Also, moment frames and their shear frame counterparts are considered and compared for optimal design. The results indicate a good performance of the proposed algorithm to find an optimal solution for 3D RC frames.

Keywords: 3D Reinforced concrete frames; Structural optimization; Improved plasma generation optimization (IPGO) algorithm; Metaheuristics.

1. Introduction

Optimal design of steel structures is generally considered the minimum weight, construction cost of the members, and maximum stiffness while the reinforced concrete structures have multi-

* E-mail address of the corresponding author: alikaveh@iust.ac.ir (A. Kaveh)

materials and the objective function is obtained the construction cost of the formwork, steel and concrete [1,2]. Many researchers have recently studied the optimum design of the reinforced concrete (RC) frames using the genetic algorithm [3,4], the big bang-big crunch (BB-BC) [5], harmony search-based algorithm [6], the enhanced colliding bodies optimization (ECBO) [7,8], particle swarm optimization (PSO) algorithm [9], a combination of particle swarm optimization and multi-criterion decision-making (DMPSO) algorithm [10], etc. These studies are investigated the optimization of two-dimensional (2D) reinforced concrete frame. On the other hand, the optimal design of real-world steel frames was carried out by Kaveh et al. [11] performed optimal design of the 3D steel frames with different ductility types. Carbas [12] optimized steel frames using enhanced firefly algorithm. Aydogdu et al. [13] optimized the 3D steel frames using artificial bee colony algorithm incorporating the Levy flight distribution. Kaveh and Laknejadi [14] used a multi-objective optimization for the optimal design of large steel structures. Kazemzadeh Azad and Hasancebi [15] performed optimization of steel frames by a guided stochastic search heuristic algorithm. Kaveh et al. [16] compared two types of frames consisting of prismatic frames and non-prismatic frames and optimized the 3D steel frames.

The optimum design of real-world RC structural problems requires significant computational effort because the design methods are needed for performing the constraints imposed by design codes, architectural requirements, and predetermined section databases [17]. Since the computational effort of the real-world RC frames optimization is usually high, numerical examples of previous studies are selected from the optimization of two-dimensional (2D) reinforced concrete frames. Consequently, an optimization algorithm that satisfies design requirements and economic criteria in a reasonable time would be a valuable method for designing these structures. However, there is a limited amount of investigation on optimization associated with three-dimensional (3D) RC frames according to ACI 318. Fadaee and Grierson [18] presented the optimum design of 3D frame structures using optimality criteria. Balling and Yao [19] investigated these frames using a multi-level method. Kaveh and Behnam [20] optimized 3D multi-story RC frames using the charged system search and the enhanced charged system search. Esfandiari et al. [21] presented an algorithm combining multi-criterion decision-making and Particle Swarm Optimization (DMPSO) for an optimum design in 3D RC frames. Dehnavipour et al. [22] analyzed a six-story frame structure with the PSO algorithm according to the ACI-318 specifications. In this paper, optimum design of 3D RC frames is investigated by

improved plasma generation optimization (IPGO) algorithm. This algorithm is utilized for 2D frames and the results were satisfying [23]. The main aim of this study is to find the economical design of the 3D moment and shear frames and the results of these frames are compared. The main aim of the study is to find the economical design of the 3D frame.

In the following section, the formulation of the RC frame optimization is described. The section databases and constraints of the beams and columns are provided in Section 3. The IPGO algorithm is briefly introduced in Section 4. The numerical examples of the shear and moment frames are represented in Section 5. Finally, the concluding remarks are outlined in Section 6.

2. Formulation of the RC frame optimization

The purpose of the optimization is to minimize the objective function that can be presented as:

$$\text{Find } \{Z\} = \{z_1, z_2, \dots, z_n\} \quad z_{i,min} \leq z_i \leq z_{i,max} \quad (1)$$

$$\text{To minimize } f(\{Z\}) \quad (2)$$

$$\text{Subject to } g(\{Z\}) \leq 0 \quad j = 1, 2, \dots, n_g \quad (3)$$

Where $\{Z\}$ is the design variables; n is the number of element groups; $z_{i,min}$ and $z_{i,max}$ are the lower and upper limits of design variables. $f(\{Z\})$ presents the objective function. $g_j(\{Z\})$ denotes the design constraints and n_g is the number of the constraints. A metaheuristic algorithm cannot be used for a constrained optimization problem. Thus, the constrained problem is transformed into an unconstrained one and a penalty function $f_{penalty}(\{X\})$ is obtained from all design constraints (g_i).

$$f_{penalty}(\{Z\}) = f(\{Z\}) + \sum_{i=1}^m \vartheta_i \times \max(0, g_i) \quad (4)$$

Where m is the number of the constraints and ϑ_i is the penalty parameter corresponding to the i th constraint. The non-rigid beams are the cross-section geometry of the structural elements, which are selected from databases of the beam and column sections. Due to the optimal design of an RC frame, the objective function is the costs of the beams and columns. Hence the objective function of these structures is considered the all beams and columns costs as [24]:

$$f = \sum_{i=1}^{n_b+n_c} \{C_c b_i h_i + C_s A_{si} \gamma_s\} L_i + \sum_{i=1}^{n_b} \{C_f (b_i + 2(h_i - t_i)) + C_t b_i\} L_i + \sum_{i=1}^{n_c} \{2C_f (b_i + h_i)\} L_i \quad (5)$$

Where n_b , n_c , h , b , A_{si} , and L are the number of the beams, a number of the columns, depth and width of the sections, area of the longitudinal bars in elements, and the length of the structural elements respectively; C_s , C_f , C_c , and C_t are the unit cost of steel, formwork, concrete, and scaffolding respectively; γ_s is the steel density.

3. Formation of the section databases

The design variables consist of the cross-section dimensions and detail of the steel bars. Due to a large number of RC sections, the database of the sections is utilized for the optimization process. The beam and column databases are conformed with the design code provisions of ACI 318 [25]. The beam sections are defined as rectangular shapes. The bars of #3 to #11 are used as longitudinal bars. The width and height of the sections, number and diameter of tensile and compression of bars, tensile and compression capacity, and the cost of the length unit of the elements are presented in the beams database. The cross-sections are sorted by the increasing costs. The dimensions of the beams are varied from 350×400 to 350×1050 by a step of 50 mm. The nominal bending moment strength of a beam section and the depth of an equivalent rectangular compression block are illustrated in detail in Ref. [26]. The column database includes the dimensions of the column sections, the number and diameter of the longitudinal bars, and the cost of the length unit of the members. The column sections are square with dimensions of 250 mm × 250 mm to 1200 mm × 1200 mm, by a step of 50 mm. Also, the bars of the section are selected symmetric from four #3 bars to twenty #11 bars. SAP 2000 [27] software was used to determine the elements' demand. The requirements of the ACI 318-08 code and the algorithm of the optimization are performed in MATLAB [28] software.

4. Design constraints

4.1 Constraints of beams

In each section of flexure elements, the tensile and compression moment strength of the beams must be greater than the ultimate positive and negative moment forces of the beam sections. This constraint for the moment capacity is checked as:

$$g_{b1} = \frac{|M_u| - \phi M_n}{\phi M_n} \quad (6)$$

Where M_n and M_u are the nominal moment strength and the ultimate moment force; $\phi=0.9$ is the reduction factor. Also, the maximum and minimum values of the longitudinal bars should be investigated by:

$$A_{s,min} = \frac{\sqrt{f'_c}}{4f_y} bd \geq \frac{1.4}{f_y} bd, \quad g_{b2} = A_{s,min} - A \quad (7)$$

$$A_{s,max} = 0.85\beta_1 \frac{f'_c}{f_y} \frac{600}{600 + f_y} bd, \quad g_{b3} = A - A_{s,max} \quad (8)$$

Due to the deflection limitation, the height of the beams must be greater than the minimum height, controlled as follows:

$$h_{min} = \frac{L}{21}, \quad g_{b4} = 1 - \frac{h}{h_{min}} \quad (9)$$

The height of the compressive stress block (a) must be less than the effective depth of the beam section (d), is considered as:

$$g_{b5} = \frac{a}{d} - 1 \quad (10)$$

The spacing of the longitudinal bars (s) must be greater than the allowable spacing (s_{min}) is controlled as Eq.11 where d_b is the diameter of bars.

$$s_{min} = \max(d_b, 1in), \quad g_{b6} = 1 - \frac{s}{s_{min}} \quad (11)$$

4.2 Constraint of columns

In each section of columns, the combination of the axial and moment strength (P_n, M_n) of the columns must be greater than the ultimate axial and moment forces (P_u and M_u) of the column sections. This constraint for the capacity of the column section is checked as:

$$l_u = \sqrt{(P_u)^2 + (M_u)^2}, \quad l_n = \sqrt{(\phi P_n)^2 + (\phi M_n)^2}, \quad C_1 = \frac{l_u - l_n}{l_n} \quad (12)$$

The nominal flexural of the members in x and y directions are calculated and found the ultimate capacity of each section. MacGregor method is used to consider biaxial moment of the members [29]. This method replaces the biaxial bending with an equivalent uniaxial eccentricity, and members are designed with equivalent uniaxial moments and axial force. The sections are designed for biaxial eccentricity e_{oi} that is larger than either of the e_x and e_y . For e_x/dx greater than or equal to e_y/dy , value e_{oi} should be taken as [20]:

$$e_{oi} = e_x + \beta e_y \left(\frac{dx}{dy} \right) \quad (13)$$

Where β in the above equation is calculated as [20]:

$$\beta = \frac{\left[0.5 + \frac{P_u}{f'_c A_g} \right] (f_y + 280)}{700} \geq 0.6; \quad \frac{P_u}{f'_c A_g} \leq 0.4 \quad (14)$$

$$\beta = \frac{\left[1.3 - \frac{P_u}{f'_c A_g} \right] (f_y + 280)}{700} \geq 0.5; \quad \frac{P_u}{f'_c A_g} > 0.4 \quad (15)$$

Where A_g is the gross area of the cross-section; and dx , dy are dimensions of the cross-section along the X- and Y-axis, respectively. If $e_x/dx < e_y/dy$, then, dx and dy terms are transposed. Hence, a section is checked for the load P_u and eccentricity e_{oi} . The maximum ultimate axial forces and moments are calculated by the above analysis and are compared to the ultimate capacity of each member's section. If the forces are less than the ultimate capacity, the member section is accepted. If one of them is greater than the capacity, the selected section should be changed.

The percentage of the longitudinal bars in cross-section is limited from 1 % to 8 % of the cross-section area (A_g). These constraints of the column can be expressed as:

$$C_2 = \frac{0.01 \times A_g}{A_s} - 1 \quad (16)$$

$$C_3 = \frac{A_s}{0.08 \times A_g} - 1 \quad (17)$$

The penalty of minimum clear spacing (s_{min}) in the column is provided as:

$$s_{min} = \max(1.5d_b, 1.5in), \quad C_4 = \frac{s_{min} - s}{s_{min}} \quad (18)$$

The dimensions of the column section in the top stories should be smaller than the bottom stories, so the constraints are considered as:

$$C_5 = \frac{b_T}{b_B} - 1 \quad (19)$$

$$C_6 = \frac{h_T}{h_B} - 1 \quad (20)$$

5. A brief description of the IPGO Algorithm

The plasma generation optimization (PGO) algorithm is a newly developed population-based meta-heuristic algorithm [30] and the efficiency of PGO has been investigated through the structural optimization problem [31]. In order to improve PGO, Improved Plasma Generation Optimization (IPGO) is developed to find more reliable results. In this version of the algorithm, memory is used to save a number of the best electrons [23]. The pseudo-code of IPGO is presented in Algorithm 1 [23] and the explanation of this algorithm is presented in the following steps.

1. Initial locations: the initial locations of all electrons are randomly obtained from search space according to Eq.21, and the value of the objective function for each electron is calculated.

$$x_{i,j}^0 = x_{j,min} + rand \times (x_{j,max} - x_{j,min}) \quad i = 1, 2, \dots, n \quad j = 1, 2, \dots, d \quad (21)$$

2. Saving best results: Plasma memory (PM) is used to save the best electrons and their values of the objective function. The electrons of the PM memory are added to the population and the worst electrons are deleted. Then, electrons are sorted by their values of the objective function.

3. Step size determination: A random number is used to obtain the step size of each electron. The step size of the electron in excitation, de-excitation and ionization process is obtained by the following steps.

$$\left\{ \begin{array}{ll} \text{If } rand_1 < EDR & \text{Excitation and/or de - excitation processes} \\ \text{If } rand_1 < EDR \text{ and } rand_2 < DR & \text{De - excitation process} \\ \text{If } rand_1 \geq EDR & \text{Ionization process} \end{array} \right\} \quad (22)$$

In equations, $rand_1$ and $rand_2$ are the random numbers from the interval $[0, 1]$; EDR is excitation/de-excitation rate; DR is the de-excitation rate.

A. Excitation process

In this process, the energy level of atomic electrons increases by colliding electrons with the atom. The atomic electrons have a natural movement that is limited to the atomic orbitals. Thus, electrons with lower energy level transfer to the upper ones. This transformation can be expressed in two directions:

$$stepsize_{i,j}^{excitation} = randa \times \Delta x_{i,j} + randb \times \Delta x_{i,j} \times (1 - t) \quad (23)$$

Where $randa$ and $randb$ are the random numbers in $[0.6 + 0.1 \times t, 1.4 - 0.1 \times t]$ and $[-\delta y_{i,j}, \delta y_{i,j}]$ intervals with uniform distribution; t is calculated by $\frac{iteration}{Maximum\ iteration}$; $\Delta x_{i,j}$ and $\delta y_{i,j}$ are defined as the following equations:

$$\Delta x_{i,j} = \begin{cases} x_{i,j} - x_{rc,j} & PCost_i < PCost_{rc} \\ x_{rc,j} - x_{i,j} & PCost_i \geq PCost_{rc} \end{cases} \quad (24)$$

$$\delta y_{i,j} = \sqrt{\frac{\left| randa \times \left(\frac{x_{i,j} - x_{rc,j}}{x_{j,max} - x_{j,min}} \right)^3 - \left(\frac{x_{i,j} - x_{rc,j}}{x_{j,max} - x_{j,min}} \right)^4 \right|}{2 \times iteration}} \quad (25)$$

Where $x_{i,j}$ and $x_{rc,j}$ are the locations of two different electrons that each electron compares with a random electron ($x_{rc,j}$) except itself for increasing of energy level.

B. De-excitation process

It is possible that the excited electrons lost their energy because of the interaction with gas atoms and their locations drop down the lower levels. The step size of these electrons is calculated which are obeyed from normal distribution as:

$$stepsize_{i,K}^{de-excitation} = stepsize_{i,K}^{excitation} + rand \times (x_{K,max} - x_{K,min}) \quad (26)$$

Where $rand$ is a random number with a normal distribution (mean=0 and variance=1). DRS is the de-excitation rate of the excited electron. This parameter controls the number of electrons that can perform de-excitation process. In de-excitation process, the dimensions of the electrons are randomly selected by:

$$NDRS = ceil(DRS \times d), \quad K = randsample(d, NDRS) \quad (27)$$

Where K is an integer value from 1 to variables number that returns $NDRS$ value that is sampled uniformly.

C. Ionization process

The electron beams with High energy collide with atoms and a number of these electrons are ripped from the atom to immerse in the plasma. Due to the high energy, the immersed electrons collide with others and the atoms are excited and they change into ions. The process of the ionization is modeled by electrons with levy flight and their movement can be obtained as follows:

$$stepsize_{i,j}^{ionization} = rand \times S_{i,j} \times \Delta x_{i,j} \times (1 - t) \quad (28)$$

Where $rand$ is a random number with normal distribution; and $S_{i,j}$ can be defined as:

$$S_{i,j} = \frac{rand_1}{|rand_2|^{\frac{1}{\beta}}} \times \sigma \quad (29)$$

$$\sigma = \left(\frac{\Gamma(1+\beta) \times \sin(\frac{\pi\beta}{2})}{\Gamma(\frac{1+\beta}{2}) \times \beta \times 2^{\frac{\beta-1}{2}}} \right)^{\frac{1}{\beta}}; \quad \Gamma(x) = (x-1)! \quad (30)$$

Where β is a constant parameter equal to 1.5 in this study; $rand_1$ and $rand_2$ are random numbers with normal distribution. The step size of the electron is calculated by Eqs.23, 26 and 28, Then a new location of the electrons is generated as:

$$x_{i,j}^{iteration+1} = x_{i,j}^{iteration} + stepsize_{i,j} \quad (31)$$

In the improved version of the PGO algorithm, $\Delta x_{i,j}$ is calculated by Eq.32 for moving forward to the new position around the best electron that x_{best} is the best electron in the current iteration.

$$\Delta x_{i,j} = x_{best} - x_{i,j} \quad (32)$$

4. Checking termination condition: In each new iteration, the optimization process returns to step 2. After the predetermined number of the maximum iteration, the process of the optimization is terminated.

Algorithm 1 Pseudo-code of IPGO algorithm [23]

Begin

Set algorithm parameters (n, Max iteration, EDR, DR, DRS, nPM, ...)

Create randomly initial candidate solutions

while (terminating condition is not satisfied) **do**

for all electrons

 Check lower and upper bounds of design variables

 Evaluate the objective function of electrons

end

 Sorted population according to their objective function values in an increasing order

 Plasma memory is updated

 The population is updated

for (each of electrons) **do**

 Select the best electron among n electrons (x_{best}) and generate two random numbers [0,1]

if $rand_1 < EDR$ (Excitation process occurs)

 Generate new solution using Eqs.23 and 31

```

if rand2 < DR (De-excitation process occurs)
    Calculate NDRS and K using Eq.27.
    Changing some dimensions of the new solution using Eqs.26 and 31.
end if
else (ionization process occurs)
    Generate a new solution based on the ionization process using Eqs.28 and 31
end if
end for
end while
end

```

6. Numerical examples

In this section, four frame structures are optimized using the IPGO algorithm. Two sets of frames including moment and shear frames are studied. These are typical 3-story and 7-story RC frames in each horizontal direction [20]. The equivalent static analysis is utilized to obtain the demand of the beams and columns. Moreover, SAP2000 [27] is used for finite element analysis. The frames are optimized according to their construction cost. In all examples, the structural characteristics of the frames include a service dead load of $D=5.9 \text{ kN/m}^2$, uniform service live load of $L=2 \text{ kN/m}^2$ and lateral loads are calculated based on the ASCE7 code [32]. The two-way slab is considered for the flooring system. Lateral forces are applied at the mass center of each story. The values of the required parameter of the examples are provided in Table 1. The behavior of the materials is considered linear elastic and the load combinations are selected as:

$$U = 1.2DL + 1.6LL \quad (33)$$

$$U = 1.2DL + LL \pm 1.4EL \quad (34)$$

$$U = 0.9DL \pm 1.4EL \quad (35)$$

Table.1 Design constants [23]

	Unit	Value
Yield strength of steel (f_y)	MPa	500
Compressive strength of concrete (f_c')	Mpa	40

Unit weight of steel (γ_s)		kg/m ³	7849
Unit weight of concrete (γ_c)		kg/m ³	2450
Cost of concrete (C_c)	beam	€/m ³	105.93
	column	€/ m ³	105.17
Cost of steel (C_s)	beam	€/kg	1.3
	column	€/kg	1.3
Cost of formwork (C_f)	beam	€/ m ²	25.05
	column	€/ m ²	22.75
Cost of scaffolding (C_i)	beam	€/ m ²	38.89
	column	€/ m ²	-

6.1 Example 1: A 3-story 3D RC shear frame

In this example, the optimal design of a 3-story shear frame is executed by the IPGO algorithm. Design variables are categorized into six groups as shown in Fig. 1. The shear frame is modeled by rigid beams. 3500 iterations for IPGO are performed, but the numbers of structural analysis are taken as 105000. The optimum results of the IPGO algorithm are reported in Table 2. It should be noted that the objective function in the shear frames is the total cost of the columns and in the moment frames, it is the total cost of the frame including columns and beams. According to the results, the cost of the columns in the shear frame is 4901 Euro.

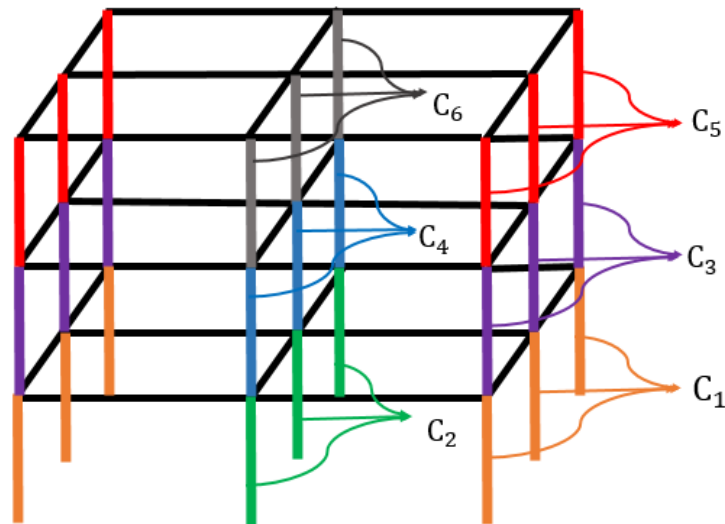


Fig. 1. 3D view of 3-story shear frames and type classification of columns

Table.2 The optimization results of the 3-story shear frame

Member type	Group	Dimensions		Reinforcements
		width (mm)	depth (mm)	
Column	C1	300	300	14#3
	C2	500	500	18#5
	C3	300	300	4#6
	C4	400	400	12#7
	C5	300	300	6#6
	C6	250	250	10#3
Total cost of columns		4901		

6.2 Example 2: A 3-story 3D RC moment frame

This example is a 3-story moment frame with two spans and 162 degrees of freedoms (DOFs). This frame has 36 beams and 27 columns arranged in 6 groups for columns and 9 groups for beams. The frame geometry and grouping details are depicted in Fig. 2. Optimal design of the frame is executed by the IPGO algorithm. For this case, the number of iterations is considered less than 3500 iterations. The results of the optimization for this case can be seen in Table 3. The results indicate that the total cost of columns and the cross-sections at the moment frame are different from those of the shear frame. The cost of the columns in the shear frame is 4901 Euro while the cost of the columns in the moment frame is 10681 Euro. Since the beams in the moment frame are considered non-rigid elements, the displacements have affected the column sections and columns with bigger cross-sections are selected in comparison to columns of the shear frame.

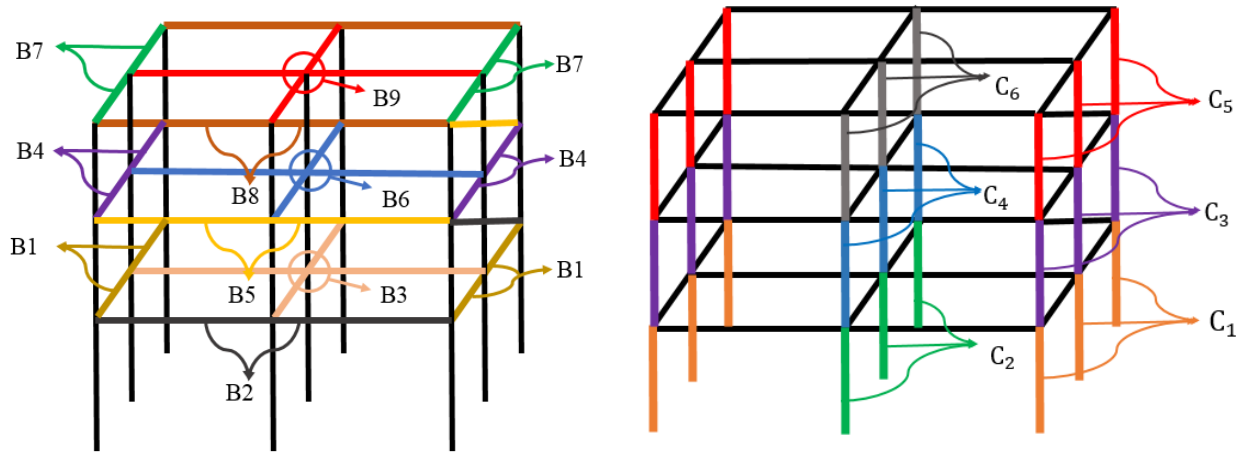


Fig. 2. 3D view of 3-story moment frames and type classification of columns and beams

Table.3 The optimization results of the 3-story moment frame

Member type	Group	Dimensions		Reinforcements	
		width (mm)	depth (mm)	As top	As bot
Beam	B1	350	400	2#4	2#3
	B2	350	400	2#4	2#3
	B3	350	400	6#4	5#4
	B4	350	400	2#4	2#3
	B5	350	400	4#3	2#3
	B6	350	400	6#6	2#9
	B7	350	400	2#4	2#3
	B8	350	400	3#5	6#3
	B9	350	400	4#5	3#6
Column	C1	950	950	10#11	
	C2	450	450	8#10	
	C3	450	450	14#5	
	C4	450	450	6#10	
	C5	350	350	8#6	
	C6	350	350	12#4	
Total cost of columns				10681	
Total cost				30179	

6.3 Example 3: A 7-story 3D RC shear frame

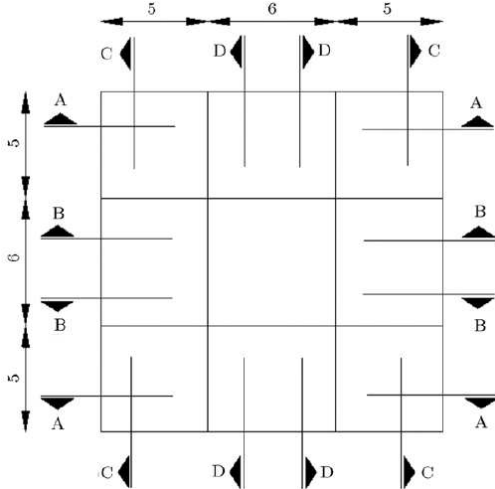
This case study is a typical 7-story RC frame with three spans in each horizontal direction. The optimal design of a shear frame is performed by the IPGO algorithm. The columns of the structure are categorized into fourteen groups. 3500 iterations for IPGO are considered and population size of 30 is used to assure the best results. The optimal sections from the IPGO algorithm are presented in Table 4. According to the results, the total cost of the columns in the shear frame is 26616 Euro.

Table.4 The optimization results of the 7-story shear frame

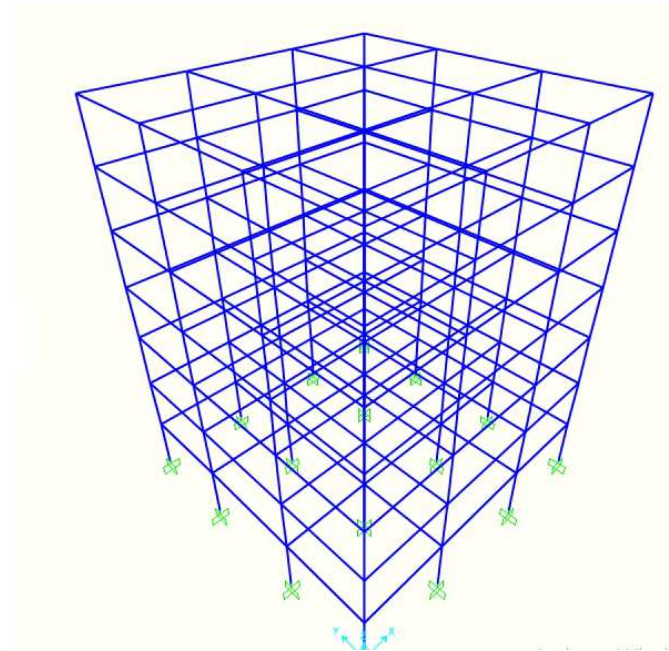
Member type	Group	Dimensions		Reinforcements	
		width (mm)	depth (mm)	As top	As bot
Column	C1	500	500	20#4	
	C2	500	500	20#4	
	C3	450	450	16#4	
	C4	500	500	14#5	
	C5	450	450	4#8	
	C6	450	450	16#4	
	C7	400	400	16#4	
	C8	450	450	16#4	
	C9	350	350	10#4	
	C10	450	450	16#4	
	C11	350	350	8#5	
	C12	450	450	4#8	
	C13	300	300	8#5	
	C14	400	400	6#6	
Total cost of columns				26616	

6.4 Example 4: A 7-story 3D RC moment frame

This example is a 7-story RC moment frame whose geometry and grouping details are shown in Fig. 3 [20]. This frame has a total of 280 members, 168 beams and 112 columns, which are arranged into 42 groups; 28 groups for beams and 14 groups for columns (Fig. 3). Beams and columns are grouped to satisfy the uniformity of the members subjected to close design forces and have similar behaviors according to their location in the frame and the loading conditions. A population size of 100 is used to assure the best results. In this example, the number of iterations of algorithms is the same as those of Example 3. The optimal sections of the optimization process are presented in Table 5 indicating that the optimum solution is feasible. In the comparison of Example 3, the stronger columns are needed for the moment frame.



Section A



Section B

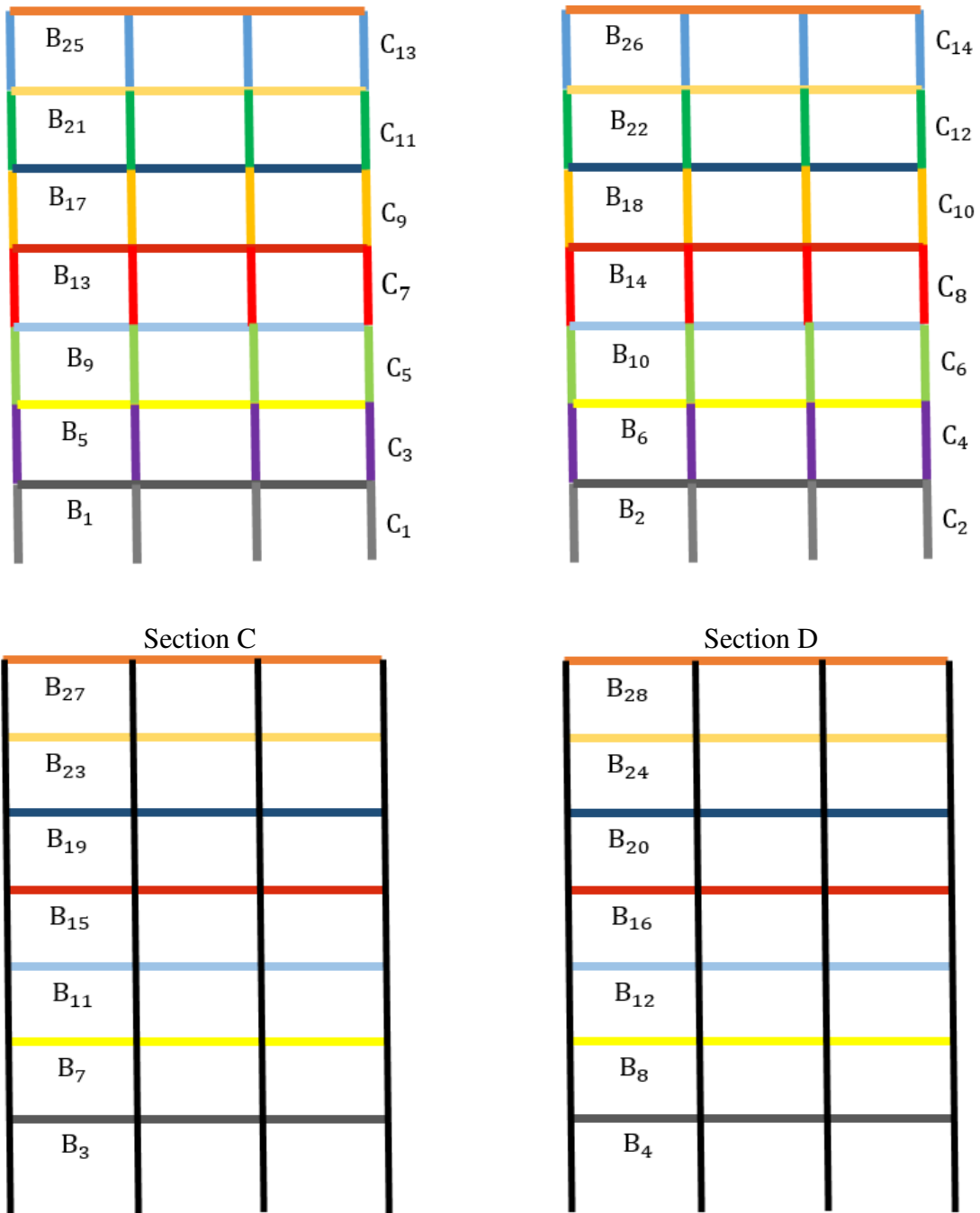


Fig 3. Plan and sections of the 7-story structure and type classification of beams and columns

Table.5 The optimization results of the 7-story frame under equivalent static analysis

Member type	Group	Dimensions		Reinforcements	
		width (mm)	depth (mm)	As top	As bot
Beam	B1	350	450	3#8	5#84

B2	350	400	3#6	4#7
B3	350	1050	4#6	2#10
B4	350	1000	4#10	5#11
B5	350	450	2#9	6#5
B6	350	500	3#9	2#9
B7	350	700	5#3	5#4
B8	350	500	2#4	3#6
B9	350	400	4#5	2#6
B10	350	450	5#8	4#5
B11	350	400	5#3	3#3
B12	350	400	4#3	2#3
B13	350	400	3#5	3#6
B14	350	400	4#5	2#6
B15	350	900	5#5	5#5
B16	350	550	2#5	5#3
B17	350	400	5#4	2#6
B18	350	400	3#4	3#4
B19	350	400	2#3	6#3
B20	350	400	2#4	2#3
B21	350	400	3#4	3#3
B22	350	600	5#6	6#9
B23	350	400	4#8	3#3
B24	350	400	4#3	5#3
B25	350	750	6#7	4#7
B26	350	550	2#11	6#3
B27	350	450	2#3	4#4
B28	350	400	6#3	4#3
C1	1200	1200	20#11	
C2	1200	1200	20#11	
C3	1000	1000	20#8	

C4	1200	1200	20#11
C5	700	700	16#8
C6	1200	1200	20#11
C7	700	700	10#10
C8	1200	1200	20#11
C9	700	700	18#6
C10	900	900	18#10
C11	400	400	16#5
C12	800	800	18#7
C13	300	300	16#4
C14	300	300	10#5
Total cost of columns		93410	
Total cost		213730	

Concluding Remarks

The optimum design of 3D RC frames is a nonlinear problem and a time-consuming procedure. Therefore, the use of an efficient optimization algorithm is vital. The algorithm should be capable of escaping the local optimums and it should converge in a sensible time. In this paper, the improved plasma generation optimization (IPGO) algorithm is selected as the optimization method. The shear and moment RC frames with different stories are designed according to the standards and requirements of the American Concrete Institute's Building Code (ACI 318-8). The objective function is the cost of the material and construction of reinforced concrete elements. Because a limited number of studies have been conducted on the optimum design of 3D RC frames, in this paper, the procedure of the optimization is tested to investigate the 3D structures. The shear and moment frames are considered to optimize. The numerical results demonstrated the difference between the results of the moment frame and shear frame. The results indicate that the columns of the moment frames are obtained bigger than the corresponding shear frames. Due to having non-rigid beams in the process of optimization of the moment frame, the displacement response of the shear frame is often less than the moment

frame. The results show that the proposed approach is feasible to find the optimum design of the 3D RC structures.

Conflicts of interest

The authors have no conflicts of interest to declare that are relevant to the content of this article.

References

- [1] Kaveh A. *Advances in Metaheuristic Algorithms for Optimal Design of Structures*. 3rd ed. Springer, Cham, Switzerland; 2021. <https://doi.org/10.1007/978-3-319-05549-7>
- [2] Hoseini Vaes SR, Asaad Samani A, Fathali MA. Optimum performance-based design of unsymmetrical 2D steel moment frame. *Soft Computing* 2022, 1-23.
<https://doi.org/10.1007/s00500-022-06927-x>
- [3] Govindaraj V, Ramasamy J. Optimum detailed design of reinforced concrete frames using genetic algorithms. *Engineering Optimization* 2007; vol. 39, no. 4, pp. 471-494.
<https://doi.org/10.1080/03052150601180767>
- [4] Chaudhuri P, Maity D. Cost optimization of rectangular RC footing using GA and UPSO. *Soft Computing* 2020; 24(2): 709-721.
<https://doi.org/10.1007/s00500-019-04437-x>
- [5] Kaveh A, Sabzi O. A comparative study of two meta-heuristic algorithms for optimum design of reinforced concrete frames. *International Journal of Civil Engineering* 2011; vol. 9, no. 3, pp. 193-206.
- [6] Akin A, Saka M. Harmony search algorithm based optimum detailed design of reinforced concrete plane frames subject to ACI 318-05 provisions. *Computers & Structures* 2015; vol. 147, pp. 79-95. <https://doi.org/10.1016/j.compstruc.2014.10.003>
- [7] Kaveh A. Cost and CO2 Emission Optimization of Reinforced Concrete Frames Using Enhanced Colliding Bodies Optimization Algorithm. *Applications of Metaheuristic Optimization Algorithms in Civil Engineering*: Springer, pp. 319-350; 2017.

https://doi.org/10.1007/978-3-319-48012-1_17

[8] Kaveh A, Mottaghi L, Izadifard R. Sustainable design of reinforced concrete frames with non-prismatic beams. *Engineering with Computers* 2020; pp. 1-18.

<https://doi.org/10.1007/s00366-020-01045-4>

[9] Gharehbaghi S, Fadaee M. Design optimization of RC frames under earthquake loads. *Iran University of Science & Technology* 2012; vol. 2, no. 4, pp. 459-477.

[10] Esfandiary M, Sheikholarefin S, Rahimi Bondarabadi H. A combination of particle swarm optimization and multi-criterion decision-making for optimum design of reinforced concrete frames. *Iran University of Science & Technology* 2016; 6(2), 245-268.

[11] Kaveh A, Ghafari MH, Gholipour Y. Optimal seismic design of 3D steel moment frames: different ductility types. *Structal Multidisciplinary Optimization* 2017; 56(6):1353–1368.

[12] Carbas S. Design optimization of steel frames using an enhanced firefly algorithm. *Eng Optimiz* 2016; 48(12):2007–2025.

[13] Aydoğdu İ, Akın A, Saka MP. Design optimization of real-world steel space frames using artificial bee colony algorithm with Levy flight distribution. *Adv Eng Softw* 2016; 92:1–14.

[14] Kaveh A, Laknejadi K, Alinejad B. Performance based multi-objective optimization of large steel structures. *Acta Mech* 2012; 223(2):355–369.

[15] Kazemzadeh Azad S, Hasançebi O. Computationally efficient discrete sizing of steel frames via guided stochastic search heuristic. *Comput Struct* 2015; 156:12–28.

[16] Kaveh A, Kabir MZ, Bohlool M. Optimum design of three-dimensional steel frames with prismatic and non-prismatic elements. *Engineering with Computers* 2020; 36(3), 1011-1027.

[17] Lagaros ND. A general purpose real-world structural design optimization computing platform. *Struct. Multidiscip. Optim* 2013; pp. 1047–1066.

[18] Fadaee, MM. Grierson, D.E. Design optimization of 3D reinforced concrete structures. *Structural Optimization* 1996; 12, pp. 127–134.

[19] Balling RJ, Yao X. Optimization of reinforced concrete frames. *Journal of Structural Engineering, ASCE* 1997; 123, pp. 193–202.

- [20] Kaveh A, Behnam AF. Design optimization of reinforced concrete 3D structures considering frequency constraints via a charged system search. *Scientia Iranica* 2013; 20(3), 387-396.
- [21] Esfandiari M, Javad, et al. Optimum design of 3D reinforced concrete frames using DMPSO algorithm. *Advances in Engineering Software* 2018. 115: 149-160.
- [22] Dehnavipour H, Mehrabani M, Fakhriyat A, Jakubczyk-Gańczyńska A. Optimization-based design of 3D reinforced concrete structures. *Journal of Soft Computing in Civil Engineering* 2019; 3(3), 95-106.
- [23] Kaveh A, Ardebili SR. An improved plasma generation optimization algorithm for optimal design of reinforced concrete frames under time-history loading. *Structures* 2021; Vol. 34, pp. 758-770.
- [24] Kaveh A, Mottaghi L, Izadifard R. Sustainable design of reinforced concrete frames with non-prismatic beams. *Engineering with Computers* 2020; pp. 1-18.
<https://doi.org/10.1007/s00366-020-01045-4>
- [25] ACI Committee. Building code requirements for structural concrete (ACI 318-08) and commentary. American Concrete Institute 2008.
- [26] Kaveh A. Cost and CO2 Emission Optimization of Reinforced Concrete Frames Using Enhanced Colliding Bodies Optimization Algorithm. *Applications of Metaheuristic Optimization Algorithms in Civil Engineering*: Springer, pp. 319-350; 2017.
https://doi.org/10.1007/978-3-319-48012-1_17
- [27] CSI (Computers and Structures Inc.). SAP2000 v12 Analysis Reference Manual. CSI, Berkeley, 2004.
- [28] I. Mathworks, "MATLAB: the language of technical computing," *Math-Works, Inc., Natick, MA*; 1998.
- [29] MacGregor JG, Wight JK, Teng S, Irawan P. Reinforced concrete: Mechanics and Design (Vol. 3). Upper Saddle River, NJ: Prentice Hall, 1997.

[30] Kaveh A, Akbari H, Hosseini SM. Plasma generation optimization: a new physically-based metaheuristic algorithm for solving constrained optimization problems. Engineering Computations 2020. <https://doi.org/10.1108/EC-05-2020-0235>

[31] Kaveh A, Hosseini SM, Zaerreza A. Size, Layout, and Topology Optimization of Skeletal Structures Using Plasma Generation Optimization. Iranian Journal of Science and Technology, Transactions of Civil Engineering 2020; 1-31. <https://doi.org/10.1007/s40996-020-00527-1>

[32] Minimum Design Loads for Buildings and Other Structures, ASCE7-05, American Society of Civil Engineers (ASCE), 2005.